Small-Signal Equivalent Circuit Modeling of a Photodetector Chip*

Miao Ang†, Li Yiqun, Wu Qiang, Cui Hailin, Huang Yongqing, Huang Hui, and Ren Xiaomin

(*Key Laboratory of Optical Communication and Lightwave Technologies of the Ministry of Education, Beijing University of Posts and Telecommunications, Beijing* 100876, *China*)

Abstract: A small-signal equivalent circuit model and the extraction techniques for photodetector chips are presented. The equivalent lumped circuit, which takes the main factors that limit a photodetector's RF performance into consideration, is first determined based on the device's physical structure. The photodetector's S parameters are then on-wafer measured, and the measured raw data are processed with further calibration. A genetic algorithm is used to fit the measured data, thereby allowing us to calculate each parameter value of the model. Experimental results show that the modeled parameters are well matched to the measurements in a frequency range from 130MHz to 20GHz, and the proposed method is proved feasible. This model can give an exact description of the photodetector chip's high frequency performance, which enables an effective circuit-level prediction for photodetector and optoelectronic integrated circuits.

Key words: small-signal equivalent circuit model of photodetector; parameter extraction; high frequency measurement; genetic algorithm

PACC: 4280S; 0620D

CLC number: TN015 **Document code**: A **Article ID**: 0253-4177(2007)12-1878-05

1 Introduction

With the rapid development of communication technology, next-generation optical communication systems operating at 40Gb/s per channel are required. Optoelectronic integrated circuits (OEIC) are very attractive because of their high integration and high-speed performance at long-wavelength (1.55μm). To exactly estimate or simulate OEIC, accurate equivalent models of discrete device chips are very important for designers[1,2]. The photodetector is one key device for OEICs. Many modelling methods have been developed to analyze the characteristics of photodetectors[3~5]. These modelling methodologies are primarily based on numerical and physical equations, e.g., the continuity equation, leading to a lack of simple equivalent circuit models for quick determination of the photodetetor's RF performance. A small-signal equivalent circuit model is computationally less demanding. It can better describe the device's "black box" behavior and be used in a complete OEIC circuit-level analysis. As an example, an optical integrated receiver may contain photodetectors, transistors, and resistances. Design and simulation of the whole receiver can be done by combining the small-signal equivalent models of individual devices in a circuit simulator.

In this paper, a small-signal equivalent model and the extraction techniques for a photodetector chip are described. First, the model is discussed based on a pin-diode structure and physical mechanisms. Second, the chip's S parameters (S_{21} and S_{22}) are measured. The measured raw data are processed with further calibration. Finally, a genetic algorithm (GA) is used to fit the measured data, whereby we can calculate each value of the proposed model. Experimental results show good agreement with the modeled data in the frequency range from 130MHz to 20GHz, and the proposed method is proved feasible and reliable.

2 Small-signal equivalent model of the photodetector chip

Small-signal equivalent circuit models aim to

* Project supported by the State Key Development Program for Basic Research of China (No. 2003CB314901), the 111 Project (No. B07005), and the Program for Changjiang Scholars and Innovative Research Team in University (No. IRT0609)

† Corresponding author. Email: angmiao@gmail.com

Received 11 May 2007, revised manuscript received 24 July 2007

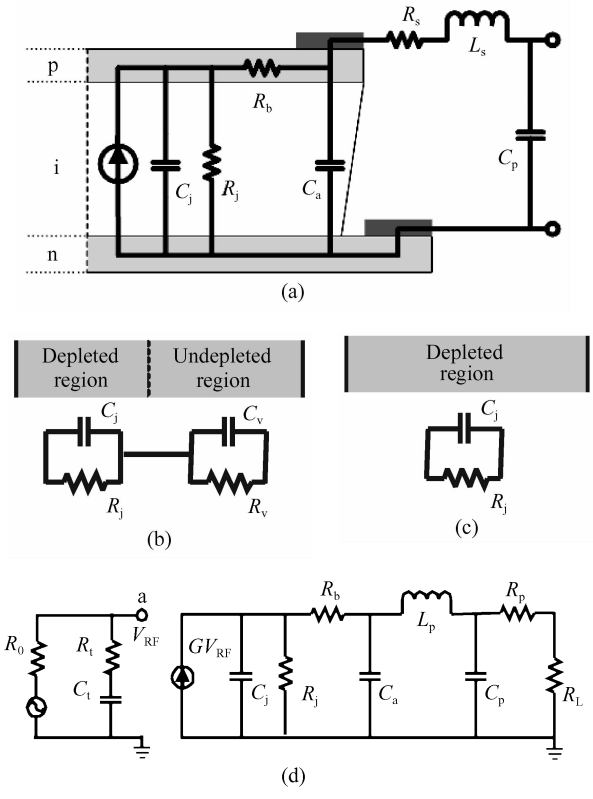

Fig. 1　Small-signal equivalent circuit model of a pin photodetector　(a) Cross section of a pin-diode; (b) Equivalent circuit of a partly depleted intrinsic region; (c) Equivalent circuit of a completely depleted intrinsic region; (d) Small-signal equivalent circuit model

simulate actual device frequency performance by circuit response, and the circuit for simulating the integrated device can be obtained by combining different models of individual devices. Figure 1 (a) shows the cross section of a pin-diode. First, we analyze the equivalent circuit model of the intrinsic region under different conditions: when applied reverse bias is not high enough to deplete the whole intrinsic region, as shown in Fig. 1 (b), the depleted region and the undepleted region can be both modeled as paralleled resistance and capacitance; When the photodetector is under normal working conditions, the intrinsic region will be completely depleted, as shown in Fig. 1 (c), and $R_v = C_v = 0$, thus the intrinsic region is modeled as parallel to R_j and C_j. The following part can be easily modeled: R_b represents the semiconductor bulk resistance of the non-depletion region; C_a represents the capacitance introduced by the top contact; the pad and interconnection line can be modeled as lump elements R_s, L_s, and C_p, similar to a circuit model of a transmission line[6].

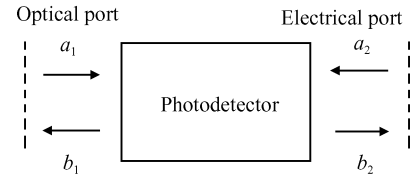

Fig. 2　Schematic showing electrical waves and optical power flowing in and out of the photodetector

To ensure the completeness of the circuit model, R_0 and R_L are included, where R_0 and R_L are the high frequency source essential resistance and load characteristic resistance, respectively, and the values are both set to 50Ω.

The model is based on the device structure, but the factors affecting device frequency response should also be taken into account. There are two main factors limiting high frequency bandwidth of photodetectors: the finite time that it takes for carriers to transit the intrinsic region and the charging and discharging time as a result of distributed resistance and capacitance. The photocurrent generated in the intrinsic region will limit the high frequency response of the photodetector as a result of the carriers' transit time, and the photocurrent's frequency dependence within the intrinsic region was described in Ref. [7]. Generally, this frequency dependence can be quite well fitted to that of an RC-link. Therefore, the photocurrent intrinsic frequency dependence can be modeled with a voltage controlled current source through the relationship $I = GV_{RF}$, where V_{RF} is the voltage at point a, as shown in Fig. 1 (d), and G is a constant adjusted according to the photodetector's quantum-efficiency. The distributed parameters above have been modeled as a lumped impedance network, which can effectively simulate the charging and discharging delay caused by the distributed parameters.

3　Accurate on-wafer measurement of photodetector chip's *S* parameters

3.1　Scattering matrices of the photodetector

For the optical port, as seen in Fig. 2, a_1 denotes the incident intensity modulated optical signal. Since no optical power travels from the right-hand side to the left across the optical port, b_1 is equal to zero. On the electrical port, a_2 and b_2 de-

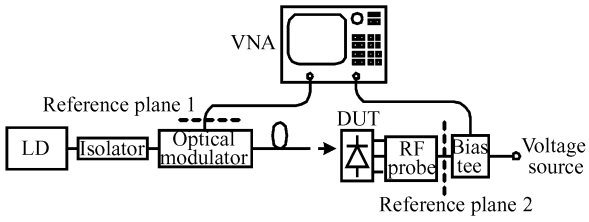

Fig. 3 Schematic graph for measurement of S_{21} (LD: Laser-diode; VNA: Vector network analyzer)

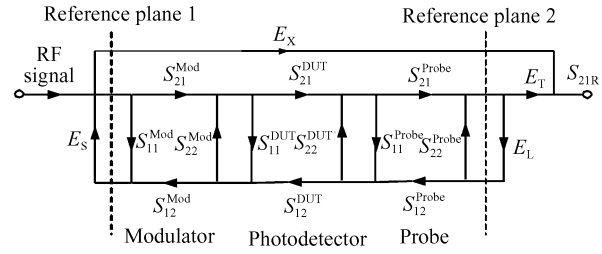

Fig. 4 Flow graph of S_{21} measurement system

note the electrical incident-wave and reflected-wave, respectively. The electrical wave b_2 has two sources: the modulated optical power incident and the electrical wave a_2 incident from the right-hand side and reflected back by the receiver's imperfect match. The photodetectors' scattering matrices can be defined as follows:

$$\begin{bmatrix} b_1 \\ b_2 \end{bmatrix} = \begin{bmatrix} 0 & 0 \\ S_{21} & S_{22} \end{bmatrix} \times \begin{bmatrix} a_1 \\ a_2 \end{bmatrix} \tag{1}$$

where S_{21} describes the amplitude of the forward electrical wave created by a_1 when $a_2 = 0$[8], and S_{22} is the electrical reflection coefficient of the photodetector's electrical output port.

3.2 Measurement and calibration of the photodetector chip's *S* parameters

To calculate model parameters from the *S* parameters, accurate on-wafer measurements of S_{21} and S_{22} are needed. S_{22} can be obtained using the one-port reflection coefficient measurement technique, which is widely used and unnecessary to explain here. S_{21} were measured using an optical - modulation technique[8]. Figure 3 shows that by connecting the DUT (device under test) and the modulated light source with a calibrated two-port vector network analyzer (VNA), we can measure S_{21} data of the DUT.

For on-wafer measurement, these procedures neglect some important errors such as modulator and microwave probe frequency response, and mismatches between ports. Measured data are inaccurate as a result of insufficient calibration, which may generate incorrect models. In order to remove the remaining errors, we have developed a "flow graph" calibration method[9]. Flow graphs are usually used in system cybernetics. Similar to system cybernetics, the propagation of microwaves is only related to the propagating path and nodes. Using a flow graph to describe microwave propagating characteristics can simplify the analysis. The flow graph of the S_{21} measurement system is shown in Fig. 4.

Furthermore, the calibrating formula is deduced based on this flow graph:

$$S_{21}^{DUT} = E(S_{21R} - E_X) \tag{2}$$

where E is the error coefficient,

$$E = \frac{(1 - S_{11}^{OE}E_S)(1 + S_{22}^{OE}E_L \times \det[S^{Probe}] - S_{22}^{Probe}E_L - S_{22}^{OE}S_{11}^{Probe})}{S_{21}^{Probe}E_T S_{21}^{Mod}} \tag{3}$$

where E_D is the directivity error, E_R is the reflection error, E_S is the source match error, E_L is the load match error, E_T is the frequency response error, E_X is the isolation error, S_{22}^{DUT} is the reflection coefficient of photodetector chip's electrical output, S_{ij}^{Probe} ($i, j = 1, 2$) are the microwave probe's *S* parameters, and S_{21R} are the measured raw data of S_{21}. Precise model parameters can be obtained with more accurate measured data. A pin-diode chip's *S* parameters were measured. Figure 5 shows that the frequency response curve of S_{21} becomes smoother after further calibration.

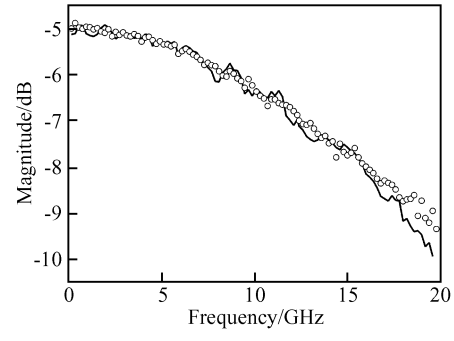

Fig. 5 Magnitude of S_{21} before and after further calibration (solid line: before calibration; dotted line: after calibration)

4 Genetic algorithm for extraction of model parameters

The extraction of the model parameters is done by fitting the calculated S parameters to the measured S parameters with GA[10~12]. GA is a stochastic optimizer that imitates the evolution of natural species toward generations with ever better average fitness. Each individual is coded as a bit string obtained by suitably joining the binary-coded values of parameters. Starting from an initial population, with the principle of survival of the fittest, through reproduction, crossover, and mutation operation, a GA continues to produce successive populations with increasing average fitness until termination conditions are satisfied. The operation is divided into the following steps:

(1) Choose proper length n of the code string: Each parameter is coded as a binary string, the minimum change step is expressed as:

(upper bound − lower bound)/$(2^n - 1)$

A more precise solution can be achieved with larger n, but when n becomes too large, operation speed will slow down. To enhance solution precision as well as operation speed, bound scopes can be reset based on preliminary results. We chose 12 as the n value.

(2) Determine the individual number N in each population: an optimum solution is difficult to achieve with small N, while convergence time is increased if N is too large. As a trade-off, we chose 60 as the N value.

(3) Create error function Y_{ELV}: Calculate each individual's fitness with the error function. Smaller Y_{ELV} values suggest better fitness. The error function is defined as follows:

$$Y_{\mathrm{ELV}} = \sum_{\text{all points}} \left(\left| \frac{S_{21\mathrm{M}} - S_{21\mathrm{C}}}{S_{21\mathrm{M}}} \right| + \left| \frac{S_{22\mathrm{M}} - S_{22\mathrm{C}}}{S_{22\mathrm{M}}} \right| \right) \tag{4}$$

where $S_{21\mathrm{M}}$ and $S_{22\mathrm{M}}$ are the measured S parameters, and $S_{21\mathrm{C}}$ and $S_{22\mathrm{C}}$ are the calculated S parameters. $S_{21\mathrm{C}}$ and $S_{22\mathrm{C}}$ are calculated as follows:

① Calculate Z parameters based on the proposed model:

$$Z_{11} = R_0 + Z_{\mathrm{t}} \tag{5}$$

$$Z_{21} = \frac{GZ_{\mathrm{t}}Z_{\mathrm{a}}Z_{\mathrm{j}}Z_{\mathrm{p}}}{(R_{\mathrm{b}} + Z_{\mathrm{j}})(Z_{\mathrm{s}} + Z_{\mathrm{p}}) + Z_{\mathrm{a}}(R_{\mathrm{b}} + Z_{\mathrm{j}} + Z_{\mathrm{s}} + Z_{\mathrm{p}})} \tag{6}$$

$$Z_{22} = \frac{Z_{\mathrm{p}}[Z_{\mathrm{s}}(R_{\mathrm{b}} + Z_{\mathrm{j}}) + Z_{\mathrm{a}}(R_{\mathrm{b}} + Z_{\mathrm{j}} + Z_{\mathrm{s}})]}{(R_{\mathrm{b}} + Z_{\mathrm{j}})(Z_{\mathrm{s}} + Z_{\mathrm{p}}) + Z_{\mathrm{a}}(R_{\mathrm{b}} + Z_{\mathrm{j}} + Z_{\mathrm{s}} + Z_{\mathrm{p}})} \tag{7}$$

where $Z_{\mathrm{t}} = R_{\mathrm{t}} + \dfrac{1}{\mathrm{j}\omega C_{\mathrm{t}}}$, $Z_{\mathrm{j}} = \dfrac{R_{\mathrm{j}}}{\mathrm{j}\omega C_{\mathrm{j}} R_{\mathrm{j}}}$, $Z_{\mathrm{a}} = \dfrac{1}{\mathrm{j}\omega C_{\mathrm{a}}}$, $Z_{\mathrm{s}} = \mathrm{j}\omega L_{\mathrm{s}} + R_{\mathrm{s}}$, $Z_{\mathrm{p}} = \dfrac{1}{\mathrm{j}\omega C_{\mathrm{p}}}$

② Transform Z parameters to S parameters, referred to as $S_{21\mathrm{C}}$ and $S_{22\mathrm{C}}$.

(4) Starting from an initial population (chosen randomly within bounds set by the user), repeat the following steps until termination conditions are satisfied:

① Calculate each individual's fitness with error function Y_{ELV};

② Based on the calculated fitness, each individual is processed through the reproduction, crossover, and mutation operation, and the individuals with the best fitness in this generation are reserved for a new population.

Table 1 shows the extracted values. Figure 6 compares the calculated S_{21} and S_{22} with the measured ones. The simulated S-parameters matched well with the measured ones over the whole investigated frequency range.

5 Conclusion

The photodetector is a key device in OEIC. To simulate its high frequency characteristics, we present a small-signal equivalent circuit model and its extraction techniques. The model is based on the photodetector's physical mechanisms and can be obtained with accurate on-wafer measured S parameters. GA is used to extract the model parameters from the measured S parameters. Experimental results show that the model approximates the measured S parameters well in the frequency range from 130MHz to 20GHz. The proposed method is proved feasible and reliable and can be used in a complete OEIC circuit-level analysis. The proposed method not only helps to simulate

Table 1　Extracted model parameters of a pin-diode chip under reverse bias of 1.5V

C_{t}	C_{j}	C_{a}	C_{p}	R_{t}	R_{j}	R_{b}	R_{s}	L_{s}	G
25.3fF	65.5fF	28.5fF	6.0fF	176.7Ω	30.8kΩ	58.5Ω	7.1Ω	18.5pH	0.0057

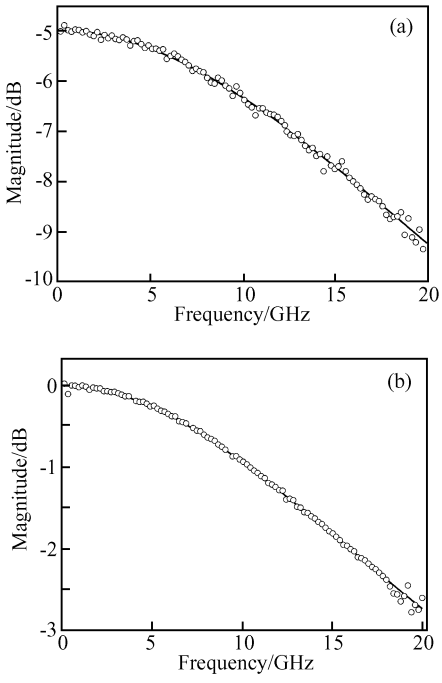

Fig. 6 Comparison between calculated and measured S parameters (solid line: the calculated; dotted line: the measured) (a) S_{21}; (b) S_{22}

and design OEICs, but also, through correlations between the model and the device, can provide a way to optimize photodetectors for high bit rate applications.

References

[1] Yang K, Gutierrez-Aitken A L, Zhang X, et al. Design, modeling, and characterization of monolithically integrated InP-based (1.55μm) high-speed (24Gb/s) p-i-n/HBT front-end photoreceivers. IEEE J Lightwave Technol, 1996, 14(8): 1831

[2] Mawby P A, Igic P M, Towers M S. Physically based compact device models for circuit modelling applications. Microelectron J, 2001, 32(5): 433

[3] Torrese G, Huynen I, Vander Vorst A. An analytical small-signal model for submicrometer n^+-i-n^+ traveling-wave photodetectors. IEEE Trans Microw Theory Tech, 2005, 53(10): 3238

[4] Kato K. Ultrawide-band/high-frequency photodetectors. IEEE Trans Microw Theory Tech, 1999, 47(7): 1265

[5] Sabella R, Merli S. Analysis of InGaAs P-I-N photodiode frequency response. IEEE J Quantum Electron, 1993, 29(3): 906

[6] Ludwing R, Bretchko P. RF circuit design: theory and applications. Beijing: Publishing House of Electronics Industry, 2005 (in Chinese) [路德维格. 射频电路设计: 理论与应用. 北京: 电子工业出版社, 2005]

[7] Lucovsky G, Schwarz R F, Emmons R B. Transit-time considerations in p-i-n diodes. J Appl Phys, 1964, 33(3): 622

[8] Hale P D, Williams D F. Calibrated measurement of optoelectronic frequency response. IEEE Trans Microw Theory Tech, 2003, 4(3): 1422

[9] Miao A, Huang Y Q, Li Y Q, et al. Application of "glow-graph" technique in measurement calibration of high frequency characteristics of photodetectors. Chinese Journal of Semiconductors, 2007, 28(3): 448 (in Chinese) [苗昂, 黄永清, 李轶群, 等. 流图法在光探测器芯片高频特性测量校准上的应用. 半导体学报, 2007, 28(3): 448]

[10] Srinivas M, Patnaik L M. Genetic algorithms: a survey. Computer, 1994, 27(6): 17

[11] Potts J C, Giddens T D, Yadav S B. The development and evaluation of an improved genetic algorithm based on migration and artificial selection. IEEE Trans Systems, Man and Cybernetics, 1994, 24(1): 73

[12] Shi Ruiying, Liu Xunchun, Qian Yongxue, et al. HBT small-signal model extraction using a improved genetic algorithm. Chinese Journal of Semiconductors, 2002, 23(9): 957 (in Chinese) [石瑞英, 刘训春, 钱永学, 等. 用改进的遗传算法从 S 参数中提取 HBT 交流小信号等效电路模型参数. 半导体学报, 2002, 23(9): 957]

光探测器芯片小信号等效电路模型的建立*

苗 昂† 李轶群 吴 强 崔海林 黄永清 黄 辉 任晓敏

(北京邮电大学光通信与光波技术教育部重点实验室, 北京 100876)

摘要: 提出了一种光探测器芯片小信号等效电路模型及其建立方法. 首先根据光探测器的物理结构确定其等效电路模型, 模型考虑了影响光探测器高频性能的主要因素. 然后精确测量了光探测器芯片的 S 参数, 通过遗传算法对测量的 S 参数进行拟合, 最终计算出模型的各个参量. 在 130MHz～20GHz 范围内的实验结果表明, 模型仿真结果与测量结果相吻合, 证明了建模方法的可靠性. 该模型有效地模拟了光探测器芯片的高频特性, 利用该模型可以对光探测器及相应光电集成器件进行电路级仿真和优化.

关键词: 光探测器小信号等效电路模型; 参数提取; 高频测试; 遗传算法

PACC: 4280S; 0620D

中图分类号: TN015 **文献标识码:** A **文章编号:** 0253-4177(2007)12-1878-05

* 国家重点基础研究发展计划 (批准号: 2003CB314901), 高等学校学科创新引智计划 (批准号: B07005) 和教育部长江学者和创新团队发展计划 (批准号: B070051RT0609) 资助项目

† 通信作者. Email: angmiao@gmail.com

2007-05-11 收到, 2007-07-24 定稿